Enhancing Blood Flow Assessment in Diffuse Correlation Spectroscopy: A Transfer Learning Approach with Noise Robustness Analysis

Xi Chen

Biomedical Engineering

University of Strathclyde

Glasgow, United Kingdom

x.chen@strath.ac.uk

Xingda Li

Biomedical Engineering

University of Strathclyde

Glasgow, United Kingdom

xingda.li@strath.ac.uk

***Abstract*—Diffuse correlation spectroscopy (DCS) is an emerging noninvasive technique that could measure the tissue blood flow by using near-infrared coherent point-source illumination to detect spectral changes. While machine learning has demonstrated significant potential for blood flow index (BFi) analysis, an open question concerning the success of this approach pertains to its robustness in scenarios involving deviations between datasets with varying Signal-to-Noise Ratios (SNRs) originating from diverse clinical applications and various setups. This study proposes a transfer learning approach, aims to assess the influence of SNRs on the generalization ability of learned features, and demonstrate the robustness for transfer learning. A synthetic dataset with varying levels of added noise related to instrument parameters is utilized as datasets. Our proposed architecture is built upon Bi-GRU as the backbone and takes advantage of the transfer learning pre-training and fine-tuning, attention mechanism, as well as feature fusion. It takes 1x64 autocorrelation curve as input and generates BFi and the correlation parameter β. The proposed model demonstrates excellent performance when transferring from high SNRs source domain datasets to target domain datasets with relatively low SNR, exhibiting enhanced fitting accuracy across different SNRs especially for low SNR datasets when compared with other fitting methods. This highlights its potential for clinical diagnosis and treatment across various scenarios under different clinical setups.**

Keywords—diffuse correlation spectroscopy, transfer learning, cerebral blood flow, generalization ability, SNR.

I. INTRODUCTION

Diffuse correlation spectroscopy (DCS) is an optical technique capable of measuring the blood flow index (BFi) by detecting changes in the scattering of near-infrared light in tissue, which are primarily caused by the motion of red blood cells. Traditionally, DCS-based BFi measurement relies on non linear fitting methods [1-4]. However, a recent advancement has been witnessed with the application of machine learning-based approaches [5-8], demonstrating significantly enhanced accuracy. All these fitting algorithms aim to match the measured/synthetic data with the analytical or numerical solutions of the diffusion equation.

Although deep learning has shown great promise for DCS measurement, the problem here is the robustness in scenarios involving deviations, which means that datasets from diverse clinical applications with various setups may have various Signal-to-Noise Ratios (SNRs). A learned fitting procedure designed for a specific set of instrument parameters would suffer from low accuracy if it is used in different practical applications, or used in a more noisy environment. They work well mostly under a common assumption: the training and validation data are drawn from the same feature space and have the similar distribution. When the distribution changes or highly affected by noise, statistical models may need to be rebuilt from scratch using newly collected training data, which is time consuming and not available for real time BFi analysis.

In this paper, inspired by the successes of ConvGRU [5], we developed a transfer learning model based on Bi-GRU architecture, leveraging knowledge from previously learned tasks to facilitate learning of new tasks with robust noise immunity. Its objective is to transfer knowledge learned from a source domain which may cover datasets for different clinical applications to a target domain using a specific setup or in a noisy environment. By incorporating pre-training and fine-tuning of transfer learning, fitting method can become more robust and transferable, enabling them to handle data or models effectively. Besides, transfer learning allows the network to quickly adapt to new DCS applications with limited target domain datasets during fine-tuning inference process without the need of re-training. We tested the performance of the proposed architecture on datasets containing different levels of noise. The main innovations of this paper includes: (a) improve the generalization ability of current fitting algorithms via assessment of fitting accuracy and (b) show the potential to use in clinical scenarios with noise where the initial data set is too large to collect and process.

II. METHODS

A. Synthetic datasets preparation

According to the theoretical models proposed by Durduran et al. [9], the light transport in highly scattered medium such as human tissue can be expressed using diffusion approximation of the radiation transport equation, then the temporal field autocorrelation function can be acquired by resolving the photon diffusion equation while the scatters are assumed to undergo Brownian (or diffusive) motion. Here the semi-infinite tissue model with extrapolation boundary conditions is used, resulting in

$$G_1(\rho, z = 0, \tau) = \frac{v}{4\pi D}\left(\frac{e^{K(\tau)r_1}}{r_1} - \frac{e^{K(\tau)r_b}}{r_b}\right) \quad (1)$$

Where ρ is the source detector separation, $D \cong {}^{v}/_{3\mu_s'}$ is the light diffusion constant, and the decay constant is $K(\tau) = \sqrt{3\mu_s'\mu_a + \alpha(\mu_s')^2\kappa_0^2(6D_B\tau)}$. Under Brownian motion assumption, $\langle r^2\rangle = 6D_B\tau$, where D_B is the effective diffusion coefficient of the moving scatters in blood. α represents the percentage of light scattering events from moving scatters, which is assumed to be 1 in all datasets here. It is found that relative changes in αD_b correspond quite well to relative changes in blood flow measured by other techniques [9]. The isotropic source is placed on $r_1 = \sqrt{(\frac{1}{\mu_s'})^2 + \rho^2}$, and the image source is placed on the $r_b = \sqrt{(2z_b + \frac{1}{\mu_s'})^2 + \rho^2}$. Here $z_b = \frac{2}{\mu_s'}\frac{1+R_{eff}}{3(1-R_{eff})}$ is the extrapolation distance from the sample boundary as determined by the mismatch in the indices of refraction. $R_{eff} = -\frac{1.4399}{n^2} + \frac{0.7099}{n} + 0.6681 + 0.0636n$ is the effective Fresnel reflection coefficient from the interface, and n is the relative refractive index.

The analytic dataset generation is based on (1), with a wavelength of *785 nm*, μ_a and μ_s' chosen as *0.19 cm*$^{-1}$ and *11.1 cm*$^{-1}$. ρ is set as *1 cm*, and n is assumed to be *1.4*, which could represent the optical characteristic of blood vessels in human brains and human arms [10].

The noise model and SNR definition used here are developed by Chao [11] and tested under several levels of noise with adjustable parameters including photon count rate I and integration time t. The standard deviation $\sigma(\tau)$ of the measured correlation function $(g_2(\tau) - 1)$ at each delay time (τ) is estimated to be

$$\sigma(\tau) = \sqrt{\frac{T}{t}}\left[\beta^2\frac{(1+e^{-2\Gamma T})(1+e^{-2\Gamma\tau})+2m(1-e^{-2\Gamma T})e^{-2\Gamma T}}{(1-e^{-2\Gamma T})} + 2\langle n\rangle^{-1}\beta(1 + e^{-2\Gamma T}) + \langle n\rangle^{-2}\beta(1 + e^{-\Gamma\tau})\right]^{1/2} \quad (2)$$

Here Γ is the decay rate where $g_1(\tau) = exp(-\Gamma\tau)$, τ is the delay time, T is the correlator bin time interval, m is the bin index, the average number of photons $\langle n\rangle$ within bin time T is $\langle n\rangle = IT$.

The noise curves were generated with the following input parameters: Γ was obtained by fitting the synthesized data from (1) or simulation results from Monte Carlo using MCX Studio with the exponentially decaying function; I is chosen from the correlator board according to [12]; T and m were calculated corresponding to τ.

SNRs are calculated as follows:

$$\mathrm{SNR} = \frac{g_2(\tau)-1}{\sigma(\tau)} \quad (3)$$

As a result, the generated noise with standard deviation $\sigma(\tau)$ decreases as τ increases, and the corresponding SNR increases as I or t increases, as expected in (2) and (3). When $t = 1\,s$, the $g_2(\tau)$ curve with Monte Carlo simulation, as well as added noise is shown in Fig. 1.

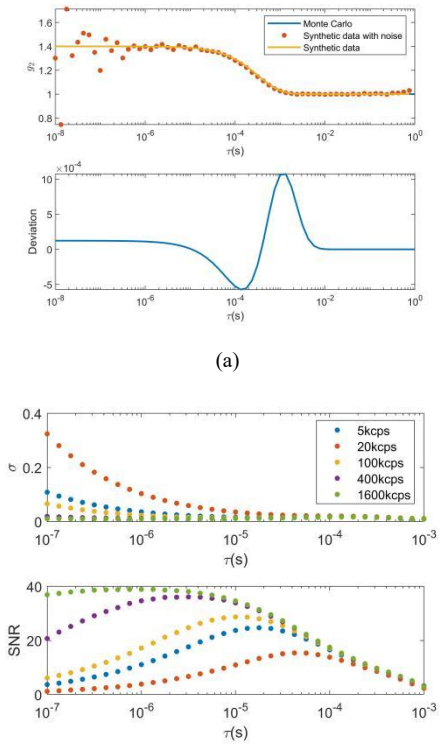

Fig 1. (a) Comparison of Monte Carlo simulation (blue solid line), analytic data (yellow solid line) and analytic data with calculated noise (dots) under $I = 60$kcps . The deviation here shows the difference of Monte Carlo simulation and analytic data. (b) Signal-to-Noise Ratio (SNR) and calculated noise for various levels. (kcps = kilo-counts per second).

For validation of the transfer learning fitting performance, three datasets with different light intensities $I = 5, 100, 400\ kcps$ respectively were generated as source and target domain datasets, representing low, medium and high SNR, respectively.

For the validation of the transferable and noise immunity ability, a mixed training datasets in source domain containing 100,000 data with BFi $\in (e^{-8}, e^{-6})$ and $\beta \in (0.01,1)$ were generated, where $I = 400 - 1600$ kcps and $t = 5 - 10$ s were used to get different $\sigma(\tau)$ and SNRs as training datasets. The target domain contains 20,000 data totally, with a ratio of training to validation is 8:2, which contained data with three low SNRs ($I = 5, 20, 100\ kcps$ and $t = 1s$) for performance evaluation in noisy environment.

B. *Transfer learning network*

The proposed transfer learning architecture is shown in Fig 2. The backbone of the architecture is Bi-directional GRU (Bi-GRU), which is stable and powerful in modeling time series input. The architecture input is $g_2(\tau)$ with a size of 1×64, while the outputs are the predicted BFi and β, each with a size of 1×1. First, a linear layer is used to increase the dimension of the input, mapping a 1D feature vector to a 3D feature vector as the input of Bi-GRU structure, which is used for sequence modeling. Compared to traditional GRU structures used in other DCS fitting algorithms [5,7], Bi-GRU leverages both past and future information for comprehensive temporal data modeling. It comprises two independent GRU networks—forward and backward—for processing sequences in both directions. Then a richer feature representation is yielded by concatenating the outputs of both networks.

Besides, while GRU resolves the gradient explosion problem in RNN, the sigmoid activation function or gate mechanism may cause information loss in intermediate features. To fully utilize the extracted features, each layer's features are extracted and fused using the torch.mean and torch.max function with the last layer's features, enhancing the utilization of source and target domain data information [13]. Unlike traditional methods that solely extract features from the final layer, this feature fusion optimally exploits complementarity among different features, preventing intermediate information loss and thereby improving model performance. Then, the torch.cat function is used again to merge the feature maps of different layers, achieving cross-level feature fusion and reducing the risk of overfitting, as well as improving the model's generalization ability.

To further enhance the model's generalization ability across different SNRs, the torch.roll function is used to roll the tensor along the given dimension, accomplishing an attention mechanism that assigns different weights to elements at different positions through displacement. In machine learning, the order of data has a certain impact on the model's training and generalization ability. The training data can be randomized by rearranging by cyclically shift the data matrix by a certain offset, thereby disrupting the data order and reduce over-fitting risk. Here the offset of -1 is set in the first dimension and -3 is chosen in the second dimension, disrupting the data for decentralization, reducing spatial features, and enhancing channel features. The acquired data is then concatenated to reduce information loss. Convolution is used to extract features, which can easily emphasize centralized features. Then, the outputs from two directions are concatenated, and the branches are then residued to prevent the loss of correlations after disruption, while maintaining the original temporal features. Finally, 1D convolution is used to extract two outputs, BFi and β. Briefly, the proposed transfer learning model establishes a direct mapping between the input 1D signal $g_2(\tau)$ and the predicted BFi and β.

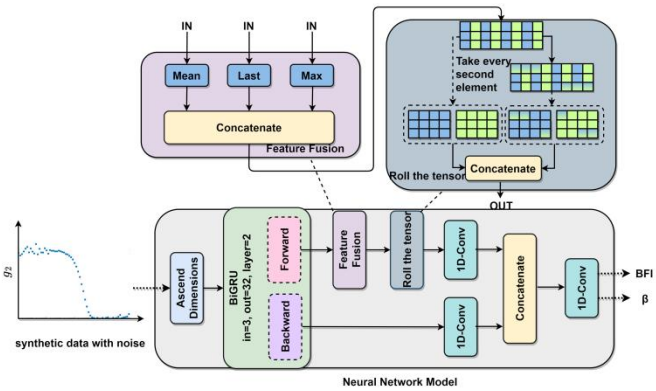

Fig 2. Structure of the proposed Transfer Learning model.

All the models are trained for 100 epochs with an early stopping mechanism. A SGD optimizer with learning rate of 0.05 and a batch size of 1000 is used. The model was implemented in python using Pytorch and trained with an NVIDIA Core Quadro RTX 5000 GPU. A combination of mean squared error (MSE) and Maximum Mean Discrepancy (MMD) is used as the loss function. We have trained all the models with the same set of hyperparameters for a fair comparison.

III. Results and Discussions

We present the quantitative results of low, medium and high SNR in Table I using the proposed transfer learning model and compared with the results acquired by the ConvGRU model and Nelda Mead algorithm. Here for ANN performance comparison, only ConvGRU is performed in training and inference, as it has been proved to outperform GRU, LSTM, GCN and Conv1D [5]. Among these datasets, the most significant improvement is observed in the low SNR dataset, whereas a relatively minor enhancement in performance is noted in the high SNR dataset.

For the low SNR dataset, the three models all reflect the lowest accuracy among the three datasets, which is in line with expectations. This level of SNR signifies a scenario in which environmental noise holds substantial significance, or

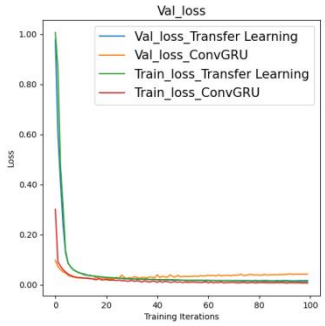

Fig 3. Loss convergence during training and inference across models.

TABLE I. Quantitative Results.

Output	indicators	Methods								
		ConvGRU			*Transfer learning*			*Nelda Mead*		
		Low SNR	***Medium SNR***	***High SNR***	***Low SNR***	***Medium SNR***	***High SNR***	***Low SNR***	***Medium SNR***	***High SNR***
BFi	R^2	0.9414	0.9504	0.9762	0.9603	0.9651	0.9824	0.8254	0.8325	0.8418
	MSE	0.0596	0.0504	0.0341	0.0405	0.0425	0.0266	0.0852	0.0702	0.0685
	MAE	0.1703	0.1609	0.1163	0.1410	0.0982	0.0807	0.2235	0.2024	0.1765
β	R^2	0.9603	0.9609	0.9964	0.9789	0.9759	0.9976	0.8498	0.8598	0.8665
	MSE	0.0392	0.0386	0.0034	0.0286	0.0020	0.0022	0.0459	0.0434	0.0421
	MAE	0.1397	0.1987	0.0438	0.1286	0.0350	0.0351	0.1964	0.2055	0.2063

the equipment is constrained, leading to a low photon count rate below 10 kHz. However, even under such conditions of low SNR, the proposed transfer learning method maintains an acceptable level of accuracy with around 2% improvement for both BFi and β compared with ConvGRU, showcasing the robustness of the proposed fitting approach. While Nelda Mead can only reach a relatively low accuracy not reliable for blood flow measurement.

For the medium SNR dataset, the gap in fitting accuracy among three fitting methods still exists but is much smaller than the case of low SNR. This level of SNR typically corresponds to instruments operating in a standard noise environment. In this SNR range, machine learning can effectively yield satisfactory fitting accuracy. However, the fitting accuracy of the Nelda Mead algorithm continues to appear unreliable.

High SNR represents an exceptionally reliable and noise-resistant environment. However, even in this scenario, the fitting accuracy of Nelda Mead is still much lower than the machine learning method. At this time, the fitting accuracy of the proposed transfer learning for BFi and β is still better than ConvGRU , although the difference is quite marginal. It is also evident that with improved SNR, the accuracy of will experience a significant enhancement.

Convergence of the training and validation loss were monitored during the training and validation process and the results are shown in Fig. 3. While both models demonstrated acceptable convergence behavior during training and validation, the transfer learning model shows a higher training loss with a lower validation noise, demonstrating its generalization ability to transfer the feature learned from high SNR training datasets in source domain to low SNR validation datasets in target domain.

IV. Conclusions

In this study, a transfer learning method for BFi quantification was investigated and evaluated. This work can provide an alternative method for continuous monitoring of BFi because of the transferable ability and noise immunity. The transfer learning model has achieved promising performance in the synthetic dataset, avoiding the iterative fitting process and improving the computational efficiency compared with traditional fitting algorithm. The results also showed that the proposed model could reach a better accuracy than the ConvGRU model for datasets with various SNRs. The most improvement showed in the low SNR, promising the anti-noise performance of transfer learning, which suggests that the transfer learning approach effectively leveraged knowledge from the pre-training phase to extract meaningful information from noisy or low-quality data. In real-world scenarios, obtaining high-quality measurements of blood flow can be challenging due to a variety of factors, including noise from physiological, environmental, and limited instrument conditions. The ability of the transfer learning model to accurately quantify BFi even under low SNR conditions is crucial for reliable and continuous monitoring of human blood flow. On the other hand, the high SNR dataset already contains relatively clean and less noisy data, leaving less room for improvement. However, even in such scenario, the transfer learning model still exhibited better compared to the ConvGRU model, which indicates the effectiveness and robustness of the transfer learning approach across the selected range of SNR levels.

References

[1] Udelhoven, Thomas, Christoph Emmerling, and Thomas Jarmer. "Quantitative analysis of soil chemical properties with diffuse reflectance spectrometry and partial least-square regression: A feasibility study." Plant and soil 251 (2003): 319-329.

[2] Lin, Wei, et al. "Diffuse correlation spectroscopy analysis implemented on a field programmable gate array." IEEE Access 7 (2019): 122503-122512.

[3] Shang, Yu, et al. "Extraction of diffuse correlation spectroscopy flow index by integration of N th-order linear model with Monte Carlo simulation." Applied physics letters 104.19 (2014): 193703.

[4] Zhang, Peng, et al. "Approaches to denoise the diffuse optical signals for tissue blood flow measurement." Biomedical optics express 9.12 (2018): 6170-6185.

[5] Feng, Jinchao, et al. "Cerebral blood flow monitoring using a ConvGRU model based on diffuse correlation spectroscopy." Infrared Physics & Technology (2023): 104541.

[6] Poon, Chien-Sing, Feixiao Long, and Ulas Sunar. "Deep learning model for ultrafast quantification of blood flow in diffuse correlation spectroscopy." Biomedical Optics Express 11.10 (2020): 5557-5564.

[7] Li, Zhe, et al. "Quantification of blood flow index in diffuse correlation spectroscopy using long short-term memory architecture." Biomedical Optics Express 12.7 (2021): 4131-4146.

[8] Zhang, Peng, et al. "Signal processing for diffuse correlation spectroscopy with recurrent neural network of deep learning." 2019 IEEE Fifth International Conference on Big Data Computing Service and Applications (BigDataService). IEEE, 2019.

[9] Durduran, T., Choe, R., Baker, W. B., & Yodh, A. G. (2010). Diffuse optics for tissue monitoring and tomography. Reports on progress in physics, 73(7), 076701.

[10] Li, J., Qiu, L., Poon, C. S., & Sunar, U. (2017). Analytical models for time-domain diffuse correlation spectroscopy for multi-layer and heterogeneous turbid media. Biomedical optics express, 8(12), 5518-5532.

[11] Zhou, Chao, et al. "Diffuse optical correlation tomography of cerebral blood flow during cortical spreading depression in rat brain." Optics express 14.3 (2006): 1125-1144.

[12] Cortese, Lorenzo, et al. "Recipes for diffuse correlation spectroscopy instrument design using commonly utilized hardware based on targets for signal-to-noise ratio and precision." Biomedical Optics Express 12.6 (2021): 3265-3281.

[13] Lin, C. J., Lin, C. H., & Jeng, S. Y. (2020). Using feature fusion and parameter optimization of dual-input convolutional neural network for face gender recognition. Applied Sciences, 10(9), 3166.